Synthesis of carbon-11-labeled CK1 inhibitors as new potential PET radiotracers for imaging of Alzheimer's disease

Mingzhang Gao, Min Wang, Qi-Huang Zheng[*]

Department of Radiology and Imaging Sciences, Indiana University School of Medicine, 1345 West 16th Street, Room 202, Indianapolis, IN 46202, USA

ABSTRACT

The reference standards methyl 3-((2,2-difluoro-5H-[1,3]dioxolo[4′,5′:4,5]benzo[1,2-d]imidazol-6-yl)carbamoyl)benzoate (**5a**) and N-(2,2-difluoro-5H-[1,3]dioxolo[4′,5′:4,5]benzo[1,2-d]imidazol-6-yl)-3-methoxybenzamide (**5c**), and their corresponding desmethylated precursors 3-((2,2-difluoro-5H-[1,3]dioxolo[4′,5′:4,5]benzo[1,2-d]imidazol-6-yl)carbamoyl)benzoic acid (**6a**) and N-(2,2-difluoro-5H-[1,3]dioxolo[4′,5′:4,5]benzo[1,2-d]imidazol-6-yl)-3-hydroxybenzamide (**6b**), were synthesized from 5-amino-2,2-difluoro-1,3-benzodioxole and 3-substituted benzoic acids in 5 and 6 steps with 33% and 11%, 30% and 7% overall chemical yield, respectively. Carbon-11-labeled casein kinase 1 (CK1) inhibitors, [^{11}C]methyl 3-((2,2-difluoro-5H-[1,3]dioxolo[4′,5′:4,5]benzo[1,2-d]imidazol-6-yl)carbamoyl)benzoate ([^{11}C]**5a**) and N-(2,2-difluoro-5H-[1,3]dioxolo[4′,5′:4,5]benzo[1,2-d]imidazol-6-yl)-3-[^{11}C]methoxybenzamide ([^{11}C]**5c**), were prepared from their O-desmethylated precursor **6a** or **6b** with [^{11}C]CH$_3$OTf through O-[^{11}C]methylation and isolated by HPLC combined with SPE in 40–45% radiochemical yield, based on [^{11}C]CO$_2$ and decay corrected to end of bombardment (EOB). The radiochemical purity was > 99%, and the molar activity (MA) at EOB was 370–740 GBq/μmol with a total synthesis time of ~40-min from EOB.

Casein kinases (CK) are serine/threonine-specific enzymes and can be divided two subtypes: casein kinase 1 (CK1) and casein kinase 2 (CK2).[1] CK1 contains at least seven isoforms (α, β, γ1, γ2, γ3, δ and ε) expressed in eukaryotic organisms, CK1 is involved in various cellular processes including membrane trafficking, circadian rhythm, cell cycle progression, chromosome segregation, apoptosis and cellular differentiation, and deregulation of CK1 activity is linked to several pathological disorders and diseases like cancer, neurodegenerative diseases such as Alzheimer's disease (AD), Parkinson's disease (PD) and amyotrophic lateral sclerosis (ALS), and inflammatory disorders.[2,3] The overexpression of CK1 has been described in the human AD brain, since CK1 leads to an increase in amyloid-β (Aβ) peptide production, and also participates in the tau fibrillization reaction pathway through phosphorylation of tau.[4,5] CK1 has become an interesting therapeutic target for AD where an urgent need for effective treatment exists, because it opens the door for the use of CK1 inhibitors as novel therapeutic approaches for AD.[6] CK1 inhibitors can prevent Aβ formation and reverse tau hyperphosphorylation in AD, and have been used to treat neurodegenerative disorders including AD.[4,5,7] Recently a new series of difluoro-dioxolo-benzoimidazol-benzamides have been developed as potent CK1 inhibitors with nanomolar inhibitory activity, these compounds exhibited significant inhibitory effects on several tumor cell lines, and their *in vitro* biological data suggested they can be as therapeutics for AD as well.[8]

AD is a complicated neurodegenerative disease in the central nervous system (CNS), the cause of AD remains unclear, and so far no any effective treatment strategy is approved for preventing, curing and slowing the progress of AD.[9] To discover more effective treatments, more accurate diagnostic tools are crucial to reveal new therapeutic targets.[10] New noninvasive diagnostic imaging modalities for AD are really needed, both to detect and monitor the evolution of this disease, and to evaluate the efficacy of treatments.[11] Advanced biomedical imaging technique positron emission tomography (PET) is one of the most widespread imaging techniques for AD, and significant progress has been made to develop PET agents for two key neuropathological substrates of AD: Aβ plaques and tau neurofibrillary tangles (NFTs).[12,13] The representative PET Aβ and tau tracers [^{11}C]PIB and [^{18}F]Amyvid ([^{18}F]AV-45);[14,15] [^{11}C]PBB3 and [^{18}F]T807 ([^{18}F]AV-1451)[16,17] are listed in Fig. 1. The development of PET imaging probes for *in vivo* detection of Alzheimer's brains is critical for early and accurate diagnosis and for the successful discovery of AD therapies.[18] The success and limitations of Aβ imaging and tau imaging have spurred efforts worldwide to develop new selective PET tracers for different imaging targets. CK1 has emerged as a new molecular imaging target of AD,[19]
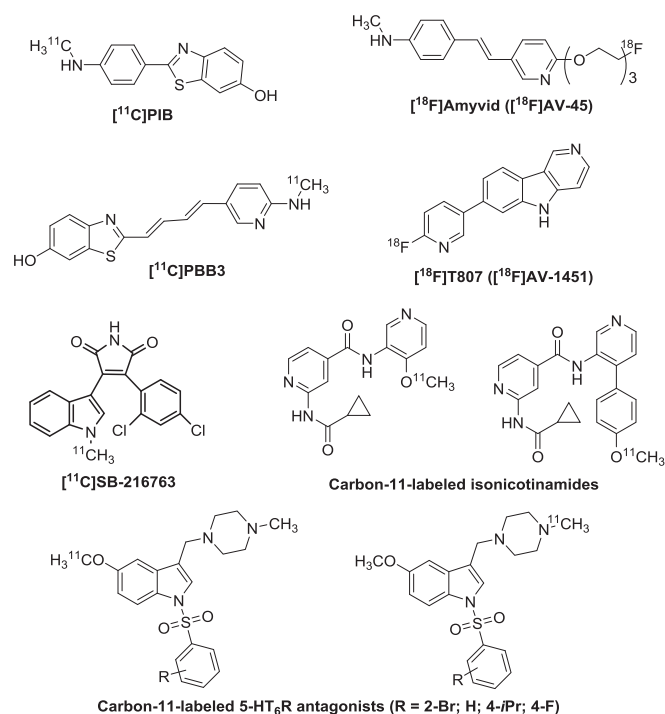
M. Gao et al.

Fig. 1. PET radiotracers for imaging of AD.

but so far no any carbon-11 or fluorine-18 labeled CK1 inhibitors as PET radiotracers for imaging of CK1 were reported. We are interested in the development of new PET AD imaging agents, and a series of enzyme- or receptor-based PET agents have been developed in this laboratory. In our previous work, we have targeted the enzyme glycogen synthase kinase-3 (GSK-3) and developed carbon-11-labeled GSK-3 inhibitors;[20,21] and we have also targeted serotonin (5-hydroxytryptamine) 6 receptor (5-HT$_6$R) and developed carbon-11-labeled 5-HT$_6$R antagonists,[22] as PET radiotracers for AD imaging (Fig. 1). In this ongoing study, we first target CK1, which is a novel and attractive molecular target for treatment and PET imaging of AD.[19] Here, we report the design, synthesis and labeling of carbon-11-labeled CK1 inhibitors, [^{11}C]methyl 3-((2,2-difluoro-5H-[1,3]dioxolo[4′,5′:4,5]benzo[1,2-d]imidazol-6-yl)carbamoyl)benzoate ([^{11}C]**5a**) and N-(2,2-difluoro-5H-[1,3]dioxolo[4′,5′:4,5]benzo[1,2-d]imidazol-6-yl)-3-[^{11}C]methoxybenzamide ([^{11}C]**5c**), as new potential PET radiotracers for imaging of AD, for the first time. The basic evaluations of the radiotracers including lipophilicity and stability are presented as well.

The reference standards methyl 3-((2,2-difluoro-5H-[1,3]dioxolo[4′,5′:4,5]benzo[1,2-d]imidazol-6-yl)carbamoyl)benzoate (**5a**) and N-(2,2-difluoro-5H-[1,3]dioxolo[4′,5′:4,5]benzo[1,2-d]imidazol-6-yl)-3-methoxybenzamide (**5c**), and their corresponding desmethylated precursors 3-((2,2-difluoro-5H-[1,3]dioxolo[4′,5′:4,5]benzo[1,2-d]imidazol-6-yl)carbamoyl)benzoic acid (**6a**) and N-(2,2-difluoro-5H-[1,3]dioxolo[4′,5′:4,5]benzo[1,2-d]imidazol-6-yl)-3-hydroxybenzamide (**6b**), were synthesized as shown in Scheme 1, according to the literature method[8] with modifications. The commercially available starting material 5-amino-2,2-difluoro-1,3-benzodioxole was treated with acetic anhydride in toluene to obtain acetamide **1** in 92% yield. Compound **1** was then converted to the intermediate **2** through a concurrent nitration and deprotection with nitronium tetrafluoroborate (NO$_2$BF$_4$) in 69% yield. In comparison with the reported method,[8] the use of the nitration reagent NO$_2$BF$_4$ simplified the reaction steps, combining nitration reaction and deprotecting reaction into one step, and improved the reaction yield. The nitro compound **2** was reduced through hydrogenation using H$_2$ and Pd/C as catalyst instead of Raney Nickel reported in the literature[8] to give the intermediate **3** containing two amino groups, which was subsequently reacted with cyanogen bromide
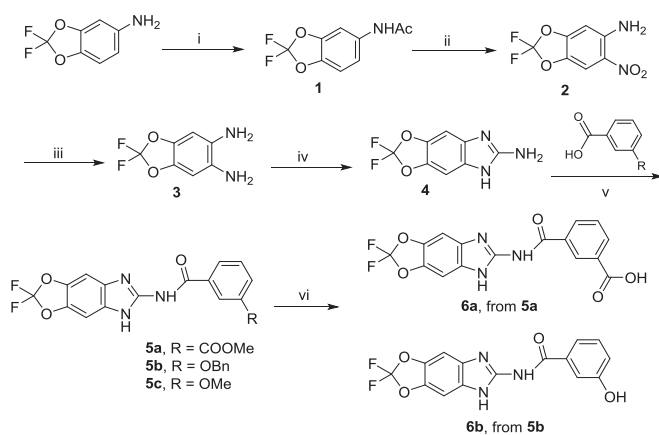

Scheme 1. Synthesis of reference standards **5a**; **5c** and O-desmethylated precursors **6a**; **6b**. Reaction reagents, conditions and yields: (i) acetic anhydride, toluene, 100 °C, 92%. (ii) NO$_2$BF$_4$, CH$_2$Cl$_2$, 69%. (iii) hydrogen, Pd/C, methanol, 82%. (iv) cyanogen bromide, methanol, room temperature (RT), 40 h, 82%. (v) 3-substitutent-benzoic acid, HBTU, DIPEA, 18–63%. (vi) for **6a**, KOH, methanol, 93%; for **6b**, Me$_2$S, BF$_3$·Et$_2$O, CH$_2$Cl$_2$, 65%.

to provide the key intermediate amino **4** in 82% yield. The catalyst change in hydrogenation also improved the yield. Then the amino **4** was reacted with several 3-substituted benzoic acids under the catalysis of $N,N,N′,N′$-tetramethyl-O-(1H-benzotriazol-1-yl)uronium hexafluorophosphate (HBTU) and N,N-diisopropylethylamine (DIPEA) to afford the standard compounds **5a** and **5c** in 63% and 21% yield, respectively. A protected benzamide **5b** was also synthesized in 18% yield. Compound **5a** was hydrolyzed in methanol solution of KOH to yield its acid precursor **6a** in 93% yield. Compound **5b** was converted to O-desmethylated precursor **6b** for compound **5c** through the deprotecting reaction of benzyl group employing boron trifluoride diethyl etherate (BF$_3$·Et$_2$O) and dimethyl sulfide (Me$_2$S) in 65% yield. This deprotective reagent system was found to be better than other deprotective reagent system like H$_2$ and Pd/C, which is easy to result in byproduct formation and lower yield.

Synthesis of the target tracers [^{11}C]**5a** and [^{11}C]**5c** is indicated in Scheme 2. O-Desmethylated precursor **6a** or **6b** underwent O-[^{11}C]methylation[23,24] using the reactive [^{11}C]methylating agent [^{11}C]methyl triflate ([^{11}C]CH$_3$OTf)[25,26] in acetonitrile at 80 °C under basic conditions (2N NaOH). The product was isolated by semi-preparative reverse-phase (RP) high performance liquid chromatography (HPLC) with a C-18 column, and then concentrated by solid-phase extraction (SPE)[27,28] with a disposable C-18 Light Sep-Pak cartridge to produce the corresponding pure radiolabeled compound [^{11}C]**5a** or [^{11}C]**5c** in 40–45% radiochemical yield, decay corrected to end of bombardment (EOB), based on [^{11}C]CO$_2$.

The radiosynthesis was performed in a home-built automated multipurpose [^{11}C]-radiosynthesis module.[29–31] Our radiosynthesis module facilitated the overall design of the reaction, purification and reformulation capabilities in a fashion suitable for adaptation to
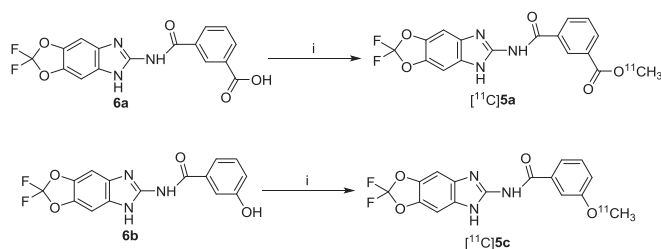
Scheme 2. Synthesis of target tracers [^{11}C]**5a** and [^{11}C]**5c**. Reaction reagents, conditions and yields: (i) [^{11}C]CH$_3$OTf, CH$_3$CN, 2 N NaOH, 80 °C, 3 min; HPLC-SPE, 40–45%.

preparation of human doses. The radiosynthesis includes three stages: 1) labeling reaction; 2) purification; and 3) formulation. More reactive [^{11}C]CH_3OTf, instead of commonly used [^{11}C]methyl iodide ([^{11}C]CH_3I),[32] was used in *O*-[^{11}C]methylation to improve radiochemical yield of [^{11}C]**5a** and [^{11}C]**5c**. The Eckert & Ziegler Modular Lab C-11 Methyl Iodide/Triflate module in our facility can produce [^{11}C]methylating agent either [^{11}C]CH_3OTf or [^{11}C]CH_3I ([^{11}C]CH_3Br passed through a NaI column). The direct comparison between [^{11}C]CH_3OTf and [^{11}C]CH_3I confirmed the result that the labeling yield was improved from 30 to 35% to 40–45%. The labeling reaction was conducted using a V-vial method. Addition of aqueous $NaHCO_3$ to quench the radiolabeling reaction and to dilute the radiolabeling mixture prior to the injection onto the semi-preparative HPLC column for purification gave better separation of [^{11}C]**5a** or [^{11}C]**5c** from its *O*-desmethylated precursor **6a** or **6b**. Both Sep-Pak trap/release and rotatory evaporation are available for formulation in our multi-purpose [^{11}C]-radiosynthesis module, and we used Sep-Pak method instead of rotatory evaporation for formulation to improve the chemical purity of radiolabeled product [^{11}C]**5a** or [^{11}C]**5c**. The direct comparison between Sep-Pak method and rotatory evaporation confirmed the result that the chemical purity of radiolabeled product was improved from < 90% to > 90%. In addition, a C18 Light Sep-Pak to replace a C18 Plus Sep-Pak allowed final product formulation with ≤5% ethanol.[33] Overall, it took ~40 min for synthesis, purification and dose formulation.

Our module is designed to allow in-process measurement of [^{11}C]-tracer molar activity (MA, GBq/μmol at EOB) using a radiation detector with a UV detector at the outlet of the HPLC-portion of the system.[31] In the HPLC chromatogram, peak analysis of the chromatographic data utilized PeakSimple software (SRI Instruments, Las Vegas, NV). Immediately following elution of the product peak, the chromatographic data are exported to PeakSimple readable files, and the area of the radioactivity peak is converted to GBq – mCi at EOB by comparison to a reference calibration curve previously constructed using the same detector, loop column, mobile phase and flow rate. The mass peak from the UV chromatogram (without decay correction) is similarly compared to a standard curve made at the same UV wavelength, mobile phase and flow rate. Simple division of the total EOB radioactivity peak (in GBq – mCi) by the total mass peak (in nmoles) gives MA at EOB in GBq – Ci/μmol. For the reported syntheses, product MA was in a range of 370–740 GBq/μmol at EOB. The factors that affect the EOB MA significantly to lead to such a wide range have been discussed in our previous works.[34–36] The general methods to increase MA have been described as well, and the MA of our [^{11}C]-tracers is significantly improved.[34–36] The 'wide range' of MA we reported is for the same [^{11}C]-tracer produced in different days, because very different [^{11}C]-target and [^{11}C]-radiosynthesis unit situations would make MA in a wide range. For a [^{11}C]-tracer produced in the same day, the MA of the same tracer in different production runs will be in a small range, because [^{11}C]-target and [^{11}C]-radiosynthesis unit would not be much different in the same day. Likewise, the methods to minimize such wide range of MA from practice perspective have been provided in our previous works.[34–36] At the end of synthesis (EOS), the MA of [^{11}C]-tracer was determined again by analytical RP HPLC, calculated, decay corrected to EOB, and based on [^{11}C]CO_2, which was in agreement with the 'on line' determined value. In this work, semi-preparative HPLC was used for purification, thus the MA of [^{11}C]-tracer was assessed by both semi-preparative HPLC (during synthesis) and analytical HPLC (EOS).

Chemical purity and radiochemical purity were determined by analytical HPLC.[37] The chemical purity of the precursor and reference standard was > 93%. The radiochemical purity of the target tracer was > 99% determined by radio-HPLC through γ-ray (PIN diode) flow detector, and the chemical purity of the target tracer was > 90% determined by reversed-phase HPLC through UV flow detector.

The octanol-water partition coefficient (commonly expressed as Log P) is an important physical parameter directly correlated with the

Table 1
Log P and CLog P values of carbon-11-labeled CK1 inhibitors [^{11}C]**5a** and [^{11}C]**5c** in comparison with [^{11}C]PIB, [^{18}F]Amyvid, [^{11}C]PBB3 and [^{18}F]T807.

Compound	Log P	CLog P
[^{11}C]**5a**	3.60	5.09
[^{11}C]**5c**	3.66	5.12
[^{11}C]PIB	3.41	3.99
[^{18}F]Amyvid	3.16	3.91
[^{11}C]PBB3	4.09	4.05
[^{18}F]T807	2.25	3.18

biological activities of a wide variety of organic compounds.[36,38] Log P provides an assessment of lipophilicity that often correlates with a compound's ability to penetrate the blood brain barrier (BBB). Log P can be determined experimentally by liquid-liquid extraction and by HPLC[38] and can also be theoretically calculated from parameters related to the structure of molecules. We obtained Log P and calculated Log P (CLog P) values of carbon-11-labeled CK1 inhibitors [^{11}C]**5a** and [^{11}C]**5c** in comparison with [^{11}C]PIB, [^{18}F]Amyvid, [^{11}C]PBB3 and [^{18}F]T807 (Fig. 1) from ChemDraw Professional 15.1 (ChemOffice), and the data are listed in Table 1. Log P data of [^{11}C]**5a** and [^{11}C]**5c** (3.60–3.66) are in the range of Log P data of [^{11}C]PIB, [^{18}F]Amyvid, [^{11}C]PBB3 and [^{18}F]T807 (2.25–4.09), which are PET AD imaging agents in clinical evaluation. These data suggest [^{11}C]**5a** and [^{11}C]**5c** have appropriate lipophilicity to pass the BBB for brain uptake.

The stability of the labeled tracers [^{11}C]**5a** and [^{11}C]**5c** was evaluated by analytical HPLC from EOS up to 3 h, one injection of the tracer solution in EtOH/saline onto HPLC column per hour. The HPLC chromatograms showed [^{11}C]**5a** and [^{11}C]**5c** were stable without decomposition.

The experimental details and characterization data for compounds **1–6** and for the tracers [^{11}C]**5a** and [^{11}C]**5c** are given.[39]

In summary, synthetic routes with moderate to high yields have been developed to produce difluoro-dioxolo-benzoimidazol-benzamides including reference standards **5a** and **5c**, and *O*-desmethylated precursors **6a** and **6b**, and carbon-11-labeled difluoro-dioxolo-benzoimidazol-benzamides target tracers [^{11}C]**5a** and [^{11}C]**5c**. The radiosynthesis employed [^{11}C]CH_3OTf for *O*-[^{11}C]methylation at *O*-desmethylated precursor, followed by product purification and isolation using a semi-preparative RP HPLC combined with SPE. [^{11}C]**5a** and [^{11}C]**5c** were obtained in high radiochemical yield, radiochemical purity and chemical purity, with a reasonable short overall synthesis time, and high molar activity. This will facilitate studies to evaluate carbon-11-labeled CK1 inhibitors [^{11}C]**5a** and [^{11}C]**5c** as new candidate PET radiotracers for imaging of AD.

Acknowledgments

References

1. Schittek B, Sinnberg T. Biological functions of casein kinase 1 isoforms and putative roles in tumorigenesis. *Mol Cancer.* 2014;13:231.
2. Vielhaber E, Virshup DM. Casein kinase I: from obscurity to center stage. *IUBMB Life.* 2001;51:73–78.
3. Rudrabhatla P. Regulation of neuronal cytoskeletal protein phosphorylation in neurodegenerative diseases. *J Alzheimer's Dis.* 2014;41:671–684.
4. Flajolet M, He G, Heiman M, Lin A, Nairn AC, Greengard P. Regulation of Alzheimer's disease amyloid-beta formation by casein kinase I. *Proc Natl Acad Sci USA.*

2007;104:4159–4164.

5. Li G, Yin H, Kuret J. Casein kinase 1 delta phosphorylates tau and disrupts its binding to microtubules. *J Biol Chem.* 2004;279:15938–15945.

6. Perez DI, Gil C, Martinez A. Protein kinases CK1 and CK2 as new targets for neuro-degenerative diseases. *Med Res Rev.* 2011;31:924–954.

7. Benek O, Hroch L, Aitken L, et al. 1-(Benzo[d]thiazol-2-yl)-3-phenylureas as dual inhibitors of casein kinase 1 and ABAD enzymes for treatment of neurodegenerative disorders. *J Enzyme Inhib Med Chem.* 2018;33:665–670.

8. Richter J, Bischof J, Zaja M, et al. Difluoro-dioxolo-benzoimidazol-benzamides as potent inhibitors of CK1δ and ε with nanomolar inhibitory activity on cancer cell proliferation. *J Med Chem.* 2014;57:7933–7946.

9. Wang M, Gao M, Zheng Q-H. The first synthesis of [¹¹C]J147, a new potential PET agent for imaging of Alzheimer's disease. *Bioorg Med Chem Lett.* 2013;23:524–527.

10. Pietrzak K, Czarnecka K, Mikiciuk-Olasik E, Szymanski P. New perspectives of Alzheimer disease diagnosis – the most popular and future methods. *Med Chem.* 2018;14:34–43.

11. Mach RH. New targets for the development of PET tracers for imaging neurode-generation in Alzheimer disease. *J Nucl Med.* 2014;55:1221–1224.

12. Hall B, Mak E, Cervenka S, Aigbirhio FI, Rowe JB, O'Brien JT. In vivo tau PET imaging in dementia: pathophysiology, radiotracer quantification, and a systematic review of clinical findings. *Ageing Res Rev.* 2017;36:50–63.

13. Oukoloff K, Cieslikiewicz-Bouet M, Chao S, et al. PET and SPECT radiotracers for Alzheimer's disease. *Curr Med Chem.* 2015;22:3278–3304.

14. Klunk WE, Engler H, Nordberg A, et al. Imaging the pathology of Alzheimer's disease: amyloid-imaging with positron emission tomography. *Neuroimaging Clin N Am.* 2003;13:781–789.

15. Carpenter Jr AP, Pontecorvo MJ, Hefti FF, Skovronsky DM. The use of the ex-ploratory IND in the evaluation and development of ¹⁸F-PET radiopharmaceuticals for amyloid imaging in the brain: a review of one company's experience. *Q J Nucl Med Mol Imaging.* 2009;53:387–393.

16. Hashimoto H, Kawamura K, Igarashi N, et al. Radiosynthesis, photoisomerization, biodistribution, and metabolite analysis of ¹¹C-PBB3 as a clinically useful PET probe for imaging of tau pathology. *J Nucl Med.* 2014;55:1532–1538.

17. Chien DT, Bahri S, Szardenings AK, et al. Early clinical PET imaging results with the novel PHF-tau radioligand [F-18]-T807. *J Alzheimers Dis.* 2013;34:457–468.

18. Okamura N, Harada R, Furukawa K, et al. Advances in the development of tau PET radiotracers and their clinical applications. *Ageing Res Rev.* 2016;30:107–113.

19. Wager TT, Galatsis P, Chandrasekaran RY, et al. Identification and profiling of a selective and brain penetrant radioligand for in vivo target occupancy measurement of casein kinase 1 (CK1) inhibitors. *ACS Chem Neurosci.* 2017;8:1995–2004.

20. Wang M, Gao M, Miller KD, Sledge GW, Hutchins GD, Zheng Q-H. The first synthesis of [¹¹C]SB-216763, a new potential PET agent for imaging of glycogen synthase kinase-3 (GSK-3). *Bioorg Med Chem Lett.* 2011;21:245–249.

21. Gao M, Wang M, Zheng Q-H. Synthesis of carbon-11-labeled isonicotinamides as new potential PET agents for imaging of GSK-3 enzyme in Alzheimer's disease. *Bioorg Med Chem Lett.* 2017;27:740–743.

22. Wang X, Dong F, Miao C, et al. Synthesis of carbon-11-labeled 5-HT₆R antagonists as new potential PET radioligands for imaging of Alzheimer's disease. *Bioorg Med Chem Lett.* 2018;28:1836–1841.

23. Wang M, Gao M, Xu Z, Zheng Q-H. Synthesis of [¹¹C]HG-10-102-01 as a new po-tential PET agent for imaging of LRRK2 enzyme in Parkinson's disease. *Bioorg Med Chem Lett.* 2017;27:1351–1355.

24. Gao M, Wang M, Meyer JA, et al. Synthesis and preliminary biological evaluation of [¹¹C]methyl (2-amino-5-(benzylthio)thiazolo[4,5-d]pyrimidin-7-yl)-d-leucinate for the fractalkine receptor (CX3CR1). *Bioorg Med Chem Lett.* 2017;27:2727–2730.

25. Jewett DM. A simple synthesis of [¹¹C]methyl triflate. *Int J Rad Appl Instrum A.* 1992;43:1383–1385.

26. Mock BH, Mulholland GK, Vavrek MT. Convenient gas phase bromination of [¹¹C] methane and production of [¹¹C]methyl triflate. *Nucl Med Biol.* 1999;26:467–471.

27. Wang M, Gao M, Miller KD, Zheng Q-H. Synthesis of [¹¹C]PBR06 and [¹⁸F]PBR06 as agents for positron emission tomography (PET) imaging of the translocator protein (TSPO). *Steroids.* 2011;76:1331–1340.

28. Wang M, Gao M, Miller KD, Sledge GW, Zheng Q-H. [¹¹C]GSK2126458 and [¹⁸F]GSK2126458, the first radiosynthesis of new potential PET agents for imaging of PI3K and mTOR in cancers. *Bioorg Med Chem Lett.* 2012;22:1569–1574.

29. Wang M, Gao M, Miller KD, Zheng Q-H. Fully automated synthesis of PET TSPO radioligands [¹¹C]DAA1106 and [¹⁸F]FEDAA1106. *Appl Radiat Isot.* 2012;70:965–973.

30. Mock BH, Zheng Q-H, DeGrado TR. A multi-purpose ¹¹C-radio-synthesis system. *J Labelled Compd Radiopharm.* 2005;48:S225.

31. Mock BH, Glick-Wilson BE, Zheng Q-H, DeGrado TR. Automated measurement of specific activity of radiolabeled ligands during synthesis. *J Labelled Compd Radiopharm.* 2005;48:S224.

32. Allard M, Fouquet E, James D, Szlosek-Pinaud M. State of art in ¹¹C labelled radio-tracers synthesis. *Curr Med Chem.* 2008;15:235–277.

33. Zheng Q-H, Glick-Wilson BE, Steele B, Shaffer M, Corbin L, Green MA. A simplified conventional manual C18 Light Sep-Pak system for purification and reformulation of carbon-11 PET tracers. *J Labelled Compd Radiopharm.* 2015;58:S392.

34. Wang M, Gao M, Xu Z, Zheng Q-H. Synthesis of a PET tau tracer [¹¹C]PBB3 for imaging of Alzheimer's disease. *Bioorg Med Chem Lett.* 2015;25:4587–4592.

35. Gao M, Wang M, Green MA, Hutchins GD, Zheng Q-H. Synthesis of [¹¹C]GSK1482160 as a new PET agent for targeting P2X₇ receptor. *Bioorg Med Chem Lett.* 2015;25:1965–1970.

36. Gao M, Wang M, Zheng Q-H. Synthesis of [¹¹C]MK-1064 as a new PET radioligand for imaging of orexin-2 receptor. *Bioorg Med Chem Lett.* 2016;26:3694–3699.

37. Zheng Q-H, Mock BH. Purification of carbon-11 PET radiotracers from unlabeled precursors by preparative HPLC and SPE. *Biomed Chromatogr.* 2005;19:671–676.

38. Liu X, Wang JQ, Zheng Q-H. Lipophilicity coefficients of potential tumor imaging agents, positron-labeled O⁶-benzylguanine derivatives. *Biomed Chromatogr.* 2005;19:379–384.

39. (a). *General:* All commercial reagents and solvents were purchased from Sigma-Aldrich and Fisher Scientific, and used without further purification. [¹¹C]CH₃OTf was prepared according to a literature procedure.[26] Melting points were determined on WRR apparatus and were uncorrected. ¹H and ¹³C NMR spectra were recorded on a Bruker Avance II 500 MHz NMR Fourier transform spectrometer at 500 and 125 MHz, respectively. Chemical shifts (δ) are reported in parts per million (ppm) relative to an internal standard tetramethylsilane (TMS, 0.0) (¹H NMR) and to the solvent signal (¹³C NMR), and coupling constants (J) are reported in hertz (Hz). Liquid chromatography-mass spectra (LC–MS) analysis was performed on an Agilent system, consisting of an 1100 series HPLC connected to a diode array detector and a 1946D mass spectrometer configured for po-sitive-ion/negative-ion electrospray ionization. The high resolution mass spectra (HRMS) were obtained using a Waters/Micromass LCT Classic spectrometer. Chromatographic solvent proportions are indicated as volume: volume ratio. Thin-layer chromatography (TLC) was run using Analtech silica gel GF uniplates (5×10 cm²). Plates were visualized under UV light. Normal phase flash column chromatography was carried out on EM Science silica gel 60 (230–400 mesh) with a forced flow of the indicated solvent system in the proportions described below. All moisture- and air-sensitive reactions were performed under a positive pressure of nitrogen maintained by a direct line from a nitrogen source. Analytical RP HPLC was performed using a Prodigy (Phenomenex) 5 μm C-18 column, 4.6×250 mm; mobile phase 60%CH₃CN/40% H₂O; flow rate 1.3 mL/min; UV (254 nm) and γ-ray (PIN diode) flow detectors. Semi-preparative RP HPLC was performed using a Prodigy (Phenomenex) 5 μm C-18 column, 10×250 mm; mobile phase 60%CH₃CN/40% H₂O; flow rate 5 mL/min; UV (254 nm) and γ-ray (PIN diode) flow detectors. C18 Light Sep-Pak cartridges were obtained from Waters Corporation (Milford, MA). Sterile Millex-FG 0.2 μm filter units were obtained from Millipore Corporation (Bedford, MA). (b). *N-(2,2-Difluorobenzo[d][1,3]dioxol-5-yl)acetamide* (**1**): A solution of 5-amino-2,2-difluoro-1,3-benzodioxole (14.4 g, 83.2 mmol) in dry toluene (230 mL) and acetic anhydride (9.76 g, 95.7 mmol, 1.15 equiv) was stirred at 100 °C for 3 h. The solvent was removed under reduced pressure, then the crude product was dissolved in 80 mL of methanol to remove traces of acetic anhydride. The solvent was subsequently evaporated. The crude product was recrystallized from toluene, and the resulting product was filtered off and dried to give a beige crystal **1** (16.5 g, 92%), $R_f = 0.25$ (1:2 EtOAc/Hexanes), mp 140–142 °C. ¹H NMR (DMSO-d₆): 2.05 (s, 3H, CH₃), 7.21 (dd, J = 2.0, 8.5 Hz, 1H, Ph−H), 7.31 (d, J = 8.5 Hz, 1H, Ph−H), 7.75 (d, J = 2.0 Hz, 1H, Ph−H), 10.14 (s, 1H, NH). MS (ESI): 216 ([M+H]⁺, 100%); MS (ESI): 214 ([M−H]⁻, 100%). (c). *2,2-Difluoro-6-nitrobenzo[d][1,3]dioxol-5-amine* (**2**): Compound **1** (15.6 g, 72.5 mmol) was dissolved in dichloromethane (250 mL). To the resulting mixture, nitronium tetrafluoroborate solu-tion (174 mL, 0.5 M in sulfolane) was added dropwise at 0 °C. After addition, the reaction mixture was allowed to RT and stirred for 24 h. Then the reaction mixture was evaporated to remove dichloromethane, and the resulting mixture was added with water, extracted with EtOAc, washed with water two times, and dried over Na₂SO₄. The mixture was filtered, and filtrate was evaporated in vacuo. The resultant residue was purified by column chromatography on silica gel with eluent (2:98 to 20:80 EtOAc/hexanes) to give a light beige solid **2** (10.9 g, 69%), $R_f = 0.73$ (CH₂Cl₂), mp 138–140 °C. ¹H NMR (DMSO-d₆): 6.94 (s, 1H, Ph−H), 7.79 (s, 2H, NH₂), 7.94 (s, 1H, Ph−H). MS (ESI): 219 ([M+H]⁺, 3%); MS (ESI): 217 ([M−H]⁻, 100%). (d). *2,2-Difluorobenzo[d][1,3]dioxole-5,6-diamine* (**3**): Compound **2** (5.0 g, 22.9 mmol) was dissolved in methanol (120 mL) and hydro-genated under hydrogen atmosphere (55 psi) with Pd/C (300–500 mg) as a catalyst for 4 h. The reaction mixture was filtered over Celite 545 and washed with methanol. The solvent step evaporated in vacuo to obtain a purple solid **3**, which was directly used for next step without further purification because this compound was unstable on silica gel column. $R_f = 0.34$ (CH₂Cl₂). MS (ESI): 189 ([M+H]⁺, 100%); MS (ESI): 187 ([M−H]⁻, 45%). (e). *2,2-Difluoro-5H-[1,3]dioxolo[4',5':4,5]benzo[1,2-d]imidazol-6-amine* (**4**): The crude product **3** (0.94 g, 5.0 mmol) was dissolved in dry methanol, cyanogen bromide (795 mg, 7.5 mmol) was added. The reaction mixture was stirred at RT for 40 h. The reaction mixture was concentrated, and the residue was purified by column chromato-graphy on silica gel with eluent (2:98 to 10:90 MeOH/CH₂Cl₂) to give a brown solid **4** (875 mg, 82%), $R_f = 0.27$ (1:19 MeOH/CH₂Cl₂), mp 135–137 °C. ¹H NMR (DMSO-d₆): 7.35 (s, 2H, Ph−H), 7.66 (s, 2H, NH₂). MS (ESI): 214 ([M+H]⁺, 100%); MS (ESI): 212 ([M−H]⁻, 70%). (f). *General procedure for synthesis of compounds 5a-c:* Compound **4** (213 mg, 1.0 mmol) and 3-substituted benzoic acid (1.0 mmol) were dissolved in 10 mL of dry *N,N*-dimethylformamide (DMF), HBTU (417 mg, 1.1 mmol) and DIPEA (258 mg, 2.0 mmol) were added, and the reaction mixture was stirred at RT for 18 h. Then the reaction mixture was concentrated in vacuo. The residue was washed with water, and dried in air to give crude product, which was purified by column chromatography on silica gel with eluent (1:99 to 5:95 MeOH/CH₂Cl₂) to afford a white solid **5**. *Methyl 3-((2,2-difluoro-5H-[1,3]dioxolo[4',5':4,5]benzo[1,2-d]imidazol-6-yl)carbamoyl)benzoate* (**5a**): Yield 63%, $R_f = 0.52$ (1:13 MeOH/CH₂Cl₂), mp 252–254 °C. ¹H NMR (acetone-d₆): 3.90 (s, 3H, OCH₃), 7.35 (s, 2H, Ph−H), 7.71 (t, J = 8.0 Hz, 1H, Ph−H), 8.23 (dt, J = 1.5, 8.0 Hz, 1H, Ph−H), 8.39 (dt, J = 1.5, 8.0 Hz, 1H, Ph−H), 8.72 (t, J = 1.5 Hz, 1H, Ph−H). MS (ESI): 376 ([M+H]⁺, 25%); MS (ESI): 374 ([M−H]⁻, 100%). *3-(Ben-zyloxy)-N-(2,2-difluoro-5H-[1,3]dioxolo[4',5':4,5]benzo[1,2-d]imidazol-6-yl)benzamide* (**5b**): Yield 18%, $R_f = 0.67$ (1:9 MeOH/CH₂Cl₂), mp 221–223 °C. ¹H NMR (acetone-d₆): 7.30–7.32 (m, 3H, Ph−H), 7.33 (dt, J = 2.0, 7.0 Hz, 1H, Ph−H), 7.39 (tt, J = 1.5, 8.5 Hz, 2H, Ph−H), 7.45–7.51 (m, 3H, Ph−H), 7.76 (td, J = 1.0, 8.0 Hz, 1H, Ph−H), 7.80 (t, J = 2.0 Hz, 1H, Ph−H), 11.80 (br s, 1H, NH). MS (ESI): 424 ([M+H]⁺, 9%); MS (ESI): 422 ([M−H]⁻, 100%). *N-(2,2-Difluoro-5H-[1,3]dioxolo[4',5':4,5]benzo[1,2-d]imidazol-6-yl)-3-methoxybenzamide* (**5c**): Yield 21%, $R_f = 0.54$ (1:13 MeOH/CH₂Cl₂), mp 241–243 °C. ¹H NMR (DMSO-d₆): 3.87 (s, 3H, OCH₃), 7.21 (ddd, J = 1.0, 2.5, 8.0 Hz, 1H, Ph−H), 7.31–7.33 (br s, 2H, Ph−H), 7.47 (t, J = 8.0 Hz, 1H, Ph−H), 7.70 (t, J = 7.0 Hz, 1H, Ph−H), 7.73 (dd, J = 1.0, 1.5 Hz, 1H, Ph−H), 7.75 (td, J = 1.0, 1.5 Hz, 1H, Ph−H), 11.80 (br s, 1H, NH). MS (ESI): 348 ([M+H]⁺, 25%); MS (ESI): 346 ([M−H]⁻, 100%). (g). *3-((2,2-Difluoro-5H-[1,3]dioxolo[4',5':4,5]benzo[1,2-d]imidazol-6-yl)carbamoyl)benzoic*

acid (**6a**): Potassium hydroxide (KOH, 0.5 g, 7.6 mmol) was added into the solution of compound **5a** (375 mg, 1.0 mmol) in methanol (20 mL). The reaction mixture was stirred at RT for 15 h. Then the reaction mixture was concentrated in vacuo, and HCl (1 N) was added to adjust pH to 7. The resulting precipitate was filtered, washed with cold water, dried in air to give a white solid **6a** (336 mg, 93%), R_f = 0.20 (1:9 MeOH/CH_2Cl_2), mp > 310 °C. ^{1}H NMR (DMSO-d_6): 7.48 (s, 2H, Ph−H), 7.63 (t, J = 7.5 Hz, 1H, Ph−H), 8.16 (d, J = 7.5 Hz, 1H, Ph−H), 8.26 (d, J = 7.5 Hz, 1H, Ph−H), 12.55 (br s, 1H, OH). MS (ESI): 362 ([M+H]$^+$, 15%); MS (ESI): 360 ([M−H]$^-$, 25%). HRMS (ESI): calcd for $C_{16}H_{10}N_3O_5F_2$, 362.0589 ([M+H]$^+$), found 362.0579. (*h*). *N-(2,2-Difluoro-5H-[1,3]dioxolo[4',5':4,5]benzo[1,2-d]imidazol-6-yl)-3-hydroxybenzamide* (**6b**): BF_3·OEt_2 (0.8 mL) and Me_2S (1.0 mL) were added to a solution of compound **5b** (212 mg, 0.5 mmol) in dichloromethane (20 mL) at 0 °C. The resulting mixture was stirred at 0 °C for 2 h and at RT for 2 h. Then the reaction mixture was evaporated to dryness in vacuo. The residue was suspended in a mixture of aqueous $NaHCO_3$, and extracted with EtOAc (3 × 80 mL). The combined organic layers were washed with brine, dried over Na_2SO_4, and concentrated. The residue was purified by column chromatography on silica gel with eluent (2:98 MeOH/CH_2Cl_2) to give a white solid **6b** (109 mg, 65%), R_f = 0.50 (7:93 MeOH/CH_2Cl_2), mp 249–251 °C. ^{1}H NMR (acetone-d_6): 7.12 (ddd, J = 0.5, 2.5, 8.5 Hz, 1H, Ph−H), 7.30 (br s, 2H, Ph−H), 7.38 (t, J = 7.0 Hz, 1H, Ph−H), 7.65 (ddd, J = 0.5, 2.5, 8.5 Hz, 1H, Ph−H), 11.77 (br s, 1H, OH). ^{13}C NMR (acetone-d_6): 113.44, 115.54, 115.79, 118.49, 119.94, 120.55, 130.76, 135.39, 140.32, 143.37, 148.67, 158.61, 167.45. MS (ESI): 334 ([M+H]$^+$, 60%); MS (ESI): 332 ([M−H]$^-$, 100%). HRMS (ESI): calcd for $C_{15}H_{10}N_3O_4F_2$, 334.0639 ([M+H]$^+$), found 334.0625. (*i*) *[^{11}C]methyl 3-((2,2-difluoro-5H-[1,3]dioxolo[4',5':4,5]benzo[1,2-d]imidazol-6-yl)carbamoyl)benzoate ([^{11}C]5a) and N-(2,2-difluoro-5H-[1,3]dioxolo[4',5':4,5]benzo[1,2-d]imidazol-6-yl)-3-[^{11}C]methoxybenzamide ([^{11}C]5c):* [^{11}C]CO_2 was produced by the ^{14}N(p,α)^{11}C nuclear reaction in the small volume (9.5 cm^3) aluminum gas target provided with the Siemens RDS-111 Eclipse cyclotron. The target gas consisted of 1% oxygen in nitrogen purchased as a specialty gas from Praxair, Indianapolis, IN. Typical irradiations used for the development were 58 μA beam current and 20 min on target. The production run produced approximately 37.0 GBq of [^{11}C]CO_2 at EOB. The precursor **6a** or **6b** (0.1–0.3 mg) was dissolved in CH_3CN (300 μL). To this solution was added aqueous NaOH (2 N, 2 μL). The mixture was transferred to a small reaction vial. No-carrier-added (high molar activity) [^{11}C]CH_3OTf that was produced by the gas-phase production method[26] within 12 min from [^{11}C]CO_2 through [^{11}C]CH_4 and [^{11}C]CH_3Br with AgOTf column was passed into the reaction vial at RT until radioactivity reached a maximum (2 min), and then the reaction vial was isolated and heated at 80 °C for 3 min. The contents of the reaction vial were diluted with aqueous $NaHCO_3$ (0.1 M, 1 mL). The reaction vial was connected to a 3-mL HPLC injection loop. The labeled product mixture solution was injected onto the semi-preparative HPLC column for purification. The product [^{11}C]**5a** or [^{11}C]**5c** fraction was collected in a recovery vial containing 30 mL water. The diluted tracer solution was then passed through a C-18 Light Sep-Pak cartridge, and washed with water (3 × 10 mL). The cartridge was eluted with EtOH (3 × 0.4 mL) to release the labeled product, followed by saline (10–11 mL). The eluted product was then sterile-filtered through a Millex-FG 0.2 μm membrane into a sterile vial. Total radioactivity was assayed and total volume (10–11 mL) was noted for tracer dose dispensing. The overall synthesis time including HPLC-SPE purification and reformulation was ~ 40 min from EOB. The decay corrected radiochemical yield was 40–45%. Retention times in the analytical HPLC system were: t_R **6a** = 4.77 min, t_R **5a** = 6.13 min, t_R [^{11}C]**5a** = 6.21 min; and t_R **6b** = 4.82 min, t_R **5c** = 6.34 min, t_R [^{11}C]**5c** = 6.41 min. Retention times in the preparative HPLC system were: t_R **6a** = 5.85 min, t_R **5a** = 10.02 min, t_R [^{11}C]**5a** = 10.18 min; and t_R **6b** = 6.05 min, t_R **5c** = 10.23 min, t_R [^{11}C]**5c** = 10.38 min.